The Wave-Assisted Cusp Model: Comparison to Low-Altitude Observations

M. Yamauchi and R. Lundin

Swedish Institute of Space Physics, Box 812, S-98128 Kiruna, Sweden (yama@irf.se)

The Wave-Assisted Cusp Model: Comparison to Low-Altitude Observations

M. Yamauchi and R. Lundin

Swedish Institute of Space Physics, Box 812, S-98128 Kiruna, Sweden (yama@irf.se)

Abstract. We first briefly describe the wave-assisted cusp model according to which a standing compressional structure at the outermost portion of the high-altitude cusp produces the cusp precipitating particles from inflowing magnetosheath plasma. The model requires two realistic assumptions: (1) A direct inflow occurs in the high-altitude cusp from the magnetosheath to the plasma mantle, experiencing a change of the cross section ("Laval nozzle effect"). (2) A substantial amount of magnetospheric/ionospheric plasma is supplied to the plasma mantle ("mixture effect"). We next examine the model's predictions against the low-altitude observations. More than twenty observational cusp characteristics are well predicted by the model.
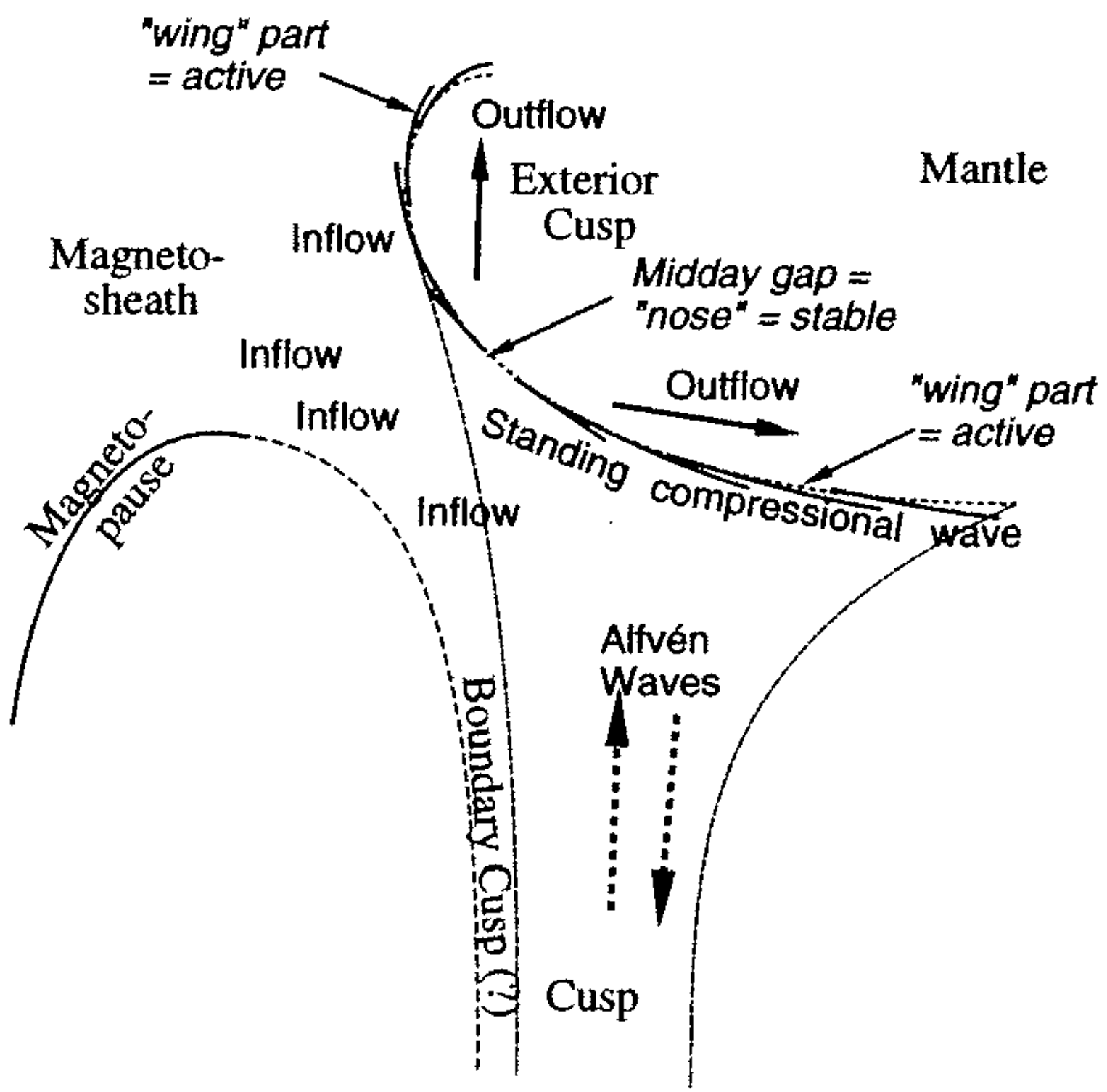
1 Introduction

The wave-assisted cusp model (or the Laval-nozzle cusp model), an alternative cusp model which is originally proposed to explain the dayside large-scale field-aligned currents (Yamauchi et al., 1993b; Yamauchi, 1994) and the multiple ion injection in the cusp (Norberg et al., 1994; Yamauchi and Lundin, 1994; Yamauchi et al., 1995), invokes a large-amplitude standing compressional wave near the high-altitude cusp as shown in Figure 1. This standing wave may be a shock. The model is still preliminary, and it requires observational as well as theoretical tests. In this paper we examine the theoretical pre-requirements for the proposed "cusp-wave," and test model predictions against low-altitude observations.

Correspondence to: M. Yamauchi

www.irf.se/%7Eyamau/papers/yamauchi1997figures

Fig. 1. Proposed standing compressional wave-like structure right above the cusp at 8-10 Re (after Yamauchi and Lundin, 1994). As an intrinsic nature of a standing wave, the "nose" part is more stable than the "wing" part. The deflection of the flow causes a strong vortex and hence isolated space charges, which help to violate the frozen-in conditions. The generation of the cusp part region 1 field-aligned currents and the "traditional" cusp currents are well explained by such a wave (Yamauchi et al., 1993a). One-two minutes' Alfvén wave transit time causes detachment of new transients every few minutes, especially when the standing structure is moving equatorward.
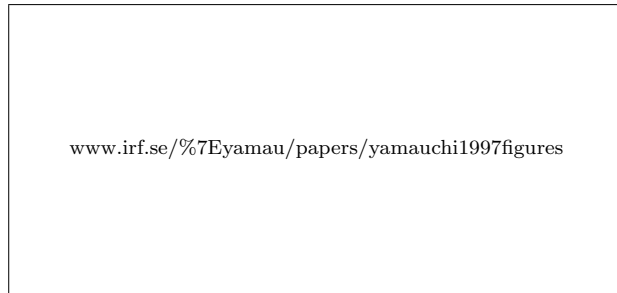
"wing" part = active

Outflow

Exterior Cusp

Mantle

Inflow

Magneto-sheath

Midday gap = "nose" = stable

Inflow

Inflow

Outflow

"wing" part = active

Magneto-pause

Standing compressional wave

Inflow

Boundary Cusp (?)

Alfvén Waves

Cusp

www.irf.se/%7Eyamau/papers/yamauchi1997figures

Fig. 2. Diagrams illustrating of cross-section areas of a "stream-tube" of a plasma flow from the magnetosheath to the plasma mantle. The cross-section area near the cusp is smaller than the area within the magnetosheath and that in the plasma mantle for the same fluid element. This provides the "Laval-nozzle effect." The magnetospheric/ionospheric plasma supply to the plasma mantle ("mixture effect") is shown by arrows. There are two successive de-Laval nozzles, one from region R_1 to region R_3, and the other from region R_3 to region R_4. We consider only the first "nozzle" where we neglect the loss of the inflow particle into the cusp in region R_2. The second nozzle may function to accelerate the mantle flow, but this is beyond the purpose of this paper. We expect the flow is subsonic in regions R_1 and R_3, and is supersonic in regions R_2 and R_4.

2 Model

Both gasdynamics and magnetohydrodynamics (MHD) predict that the magnetosheath flow will become supersonic before reaching the cusp. To have a wave or a shock in such a flow, we need a substantial obstacle downstream. It needs not to be a solid one as was imposed by Walters (1966), but could simply be a pressure increase due to, for example, the escaping magnetospheric plasma into the plasma mantle (mixture effect), while narrowing a local flow passage (or "stream tube" in fluid dynamic terminology) must be also taken into account under the cusp's special geometry as shown in Figure 2 (Laval nozzle effect).

The entire flow is analogous to a flow inside a de-Laval nozzle with finite pressure at the exit. Its flow patterns under realistic boundary conditions must be obtained only by the conservation laws of physics (mass-, momentum-, and energy-conservation) because the flow may contain a discontinuity (shock). The solutions for a neutral gas flow inside a de-Laval nozzle without magnetic fields are found in textbooks (e.g., Courant and Friedrichs, 1948, Chapter 5). Then we consider a magnetized plasma (e.g., MHD) instead of a neutral gas. This difference is small if the magnetic field does not drastically alter the conservation laws (this condition will be mentioned again later in section 3), which is the case near the magnetic cusp. Therefore, one may safely employ the regular textbook gasdynamics results to the cusp flow which experiences the de-Laval nozzle-like geometry. The effect of the magnetic field is only to add a magnetic pressure to the plasma pressure.

Figure 3 illustrates the fluid property in the de-Laval nozzle and its possible application to the high-altitude cusp. The velocity is normalized by the local characteristic speed a (we use magnetosonic speed instead of sound speed) which depends both on the temperature and on the magnetic field. We take the entrance point at the subsonic flow region inside R_1 in Figure 2 and the exit at the near-Earth plasma mantle inside R_3. The total pressure profile and the velocity profile are taken from a textbook on fluid dynamics (e.g., Courant and Friedrichs, 1948, p385). The solution depends on the exit condition. There are three classes of the solutions for the pressure and velocity profiles when the flow exists. Note that a deceleration of the solar wind does not necessarily mean a decreasing profile of the normalized velocity because the magnetic field (and hence a) decreases toward downstream.

(a) The ordinary de-Laval nozzle is designed to generate a supersonic flow. This is achieved by setting the exit pressure very low for a given cross section there (must be sufficiently large) such that the flow reaches the sound speed at the throat. The second nozzle from region R_3 to region R_4 probably obeys this solution.

(b) If the downstream pressure is sufficiently high, the flow is always subsonic (cf. the Venturi tube which uses the Bernoulli's theory to measure the flow quantities). The total pressure downstream the throat increases while decelerating the flow. Such a compressional transition is achieved without forming a shock.

(c) For certain conditions (downstream pressure is between case (a) and case (b)), the flow may first become supersonic, then form a shock, and subsequently return to subsonic again.

Generally a rarefaction case (a) is conceivable downstream the subsolar region, but with sufficient escaping ionospheric plasma into the plasma mantle the compressional solution (b) or (c) is also conceivable. We predict a discontinuity (shock) in the flow in case (c) whereas the compression is always smooth (we call "wave") in case (b). Both (b) and (c) predict a deceleration of the magnetosheath flow in the high-altitude cusp, and predict the large-amplitude wave as is illustrated in Figure 1. While the flow loses its kinetic energy, plasma heating and MHD dynamo processes take place there. The selection of the appropriate solution depends strongly on the boundary conditions ("exit" and "entrance" pressures and the shape of the "stream tube"). We thus predict a high variability of the flow. One significant boundary condition is the pressure ratio (both total and dynamic pressures) between the entrance (magnetosheath) and the exit (plasma mantle). Since the total pressure is less fluctuating in the plasma mantle than in the magnetosheath, the morphology of the high-altitude cusp must be heavily affected by the magnetosheath dynamic pressure.

The predicted compressional structure (shock or wave) is located most likely inside the high-altitude cusp because the magnetic field lines are directly connected to

acceleration

deceleration

acceleration

R_1

R_2

R_3

R_4

M'pause

Magnetospheric
Plasma Supply
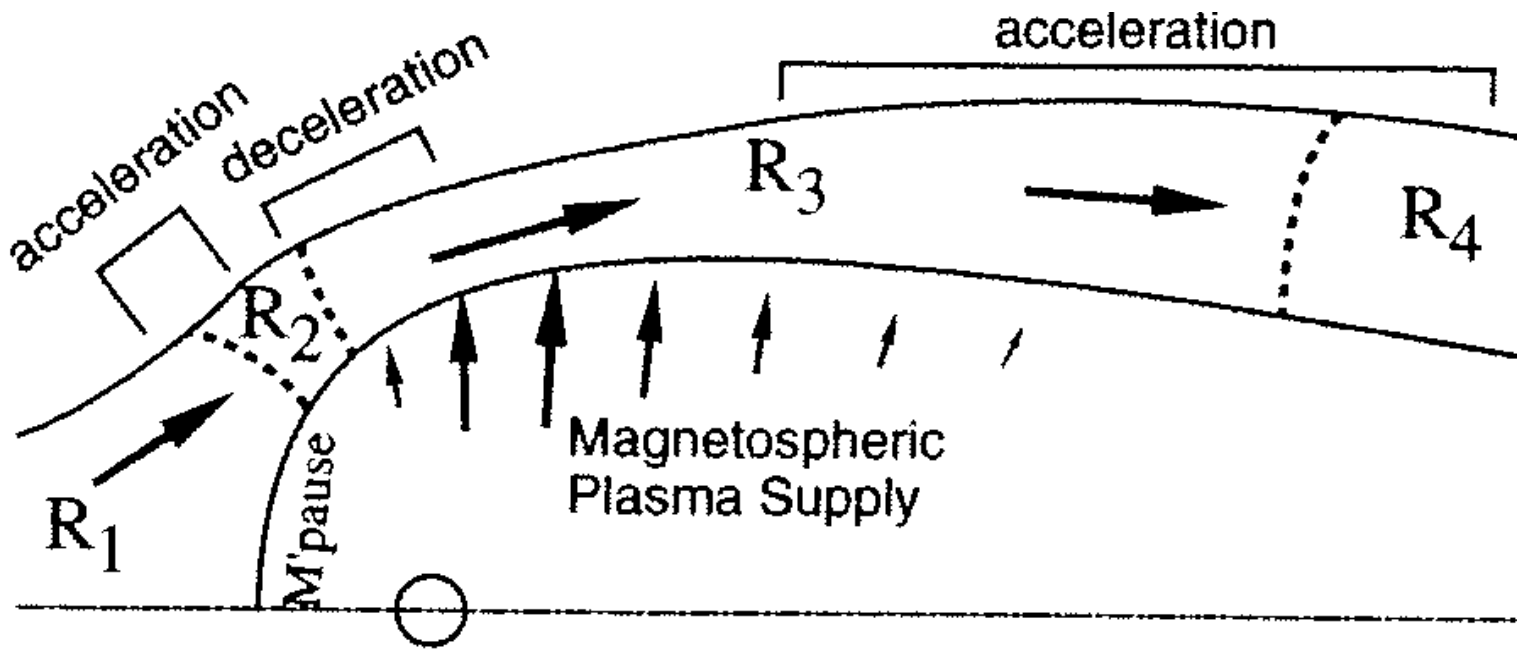
the ionosphere. The ionospheric dissipation (Joule heating) may introduce additional dissipation to the compressional structure, and it may also contribute partly to the shock formation.

3 Conditions

To have solution (b) or (c), we need (1) Narrowing of the smooth flow passage (Laval nozzle effect); and (2) Sufficient supply of magnetospheric/ionospheric plasma into the plasma mantle (mixture effect). The plasma supply is essential for the mantle formation too. In addition, the substitution of MHD fluid by neutral gas is possible only when the smooth flow exists. Thus, the model requires the following qualitative conditions:

1. The tailward plasma flow in the high-altitude cusp directly continues from the magnetosheath to the plasma mantle via high-altitude cusp.

2. A substantial amount of the magnetospheric plasma (e.g., escaped ionospheric oxygen) is supplied to the plasma mantle.

3. The magnetic tension force does not drastically alter the mass-, momentum-, and energy-conservation laws inside this direct flow.

The last condition favors to use the plasma mantle (high-latitude boundary layer) for southward IMF and the mid-latitude boundary layer for northward IMF as the downstream, because the geomagnetic field points southward in the near-cusp mantle and northward in the sub-cusp boundary layer. In fact the high-latitude boundary layer (plasma mantle) exists only during southward IMF (Sckopke et al., 1976). Therefore, we expect a drastic IMF B_z polarity dependence of the entire cusp morphology, and we limit our discussion to only the southward IMF conditions.
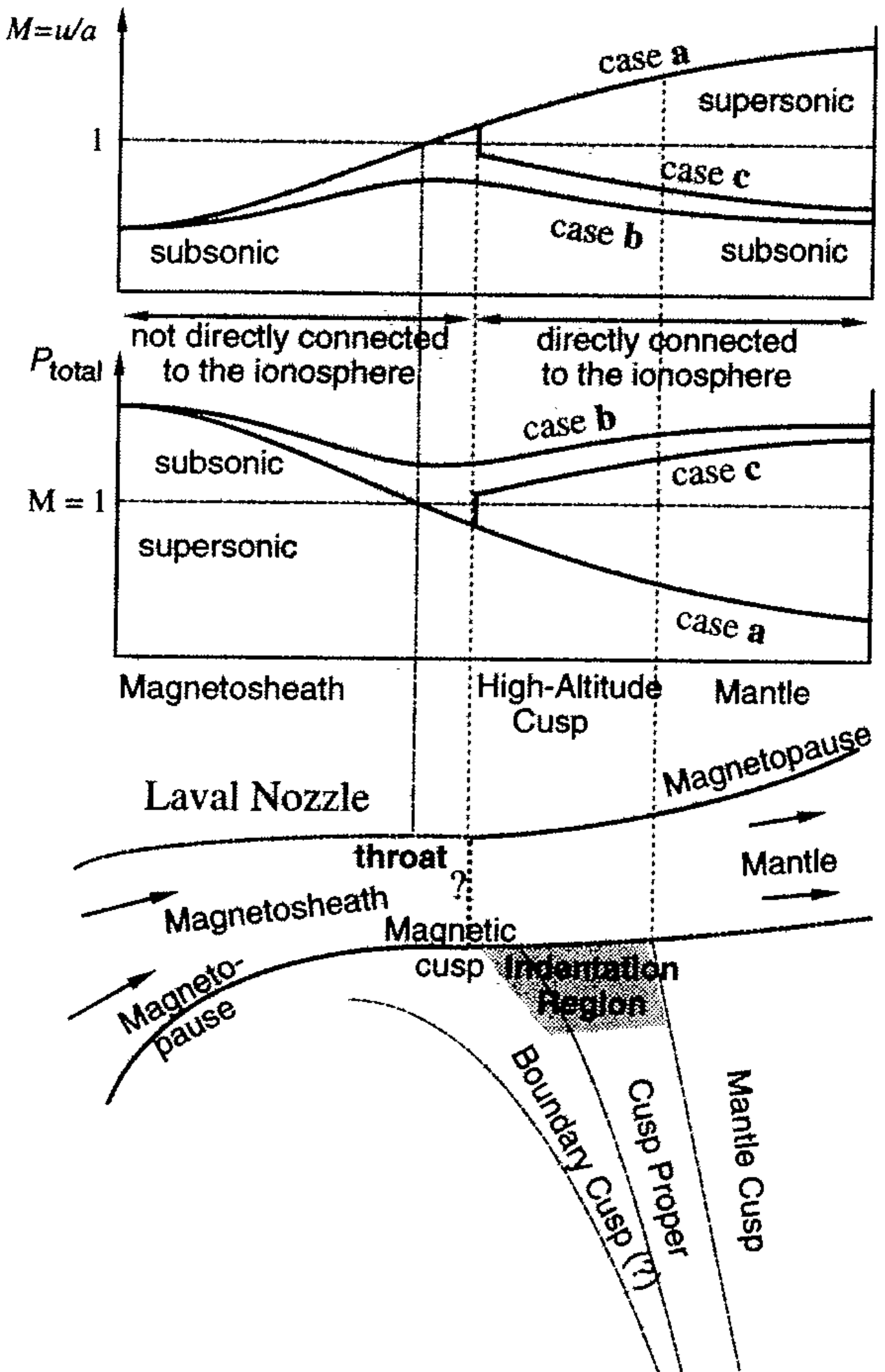
4 Predictions

We next test the anticipated cusp-wave against the low-altitude observations. As the consequences of such a magnetosonic compressional wave, we predicted the following features at low- and mid-altitudes

(a) Particle heating and flow deceleration must take place inside the compressional structure, especially at its front side. Mapping to the low-altitude, we expect higher temperature in the boundary cusp than the cusp proper, while the cusp proper is yet hotter than the magnetosheath at the topside magnetosphere. The compressional structure also naturally accompany strong waves and turbulence, and produce the precipitating particles there. The profile of the wave amplitude (or degree of heating and turbulence) may reflect the large-scale ion structure such as the energy-latitude dispersion (Burch et al., 1982; Yamauchi and Lundin, 1994), although this can also be attributed to the velocity filter effect.

www.irf.se/%7Eyamau/papers/yamauchi1997figures

Fig. 3. Diagram illustrating the cross-section area of the flow from the magnetosheath to the high-altitude cusp. The corresponding magnetospheric locations are attached in lower part. The cross section change resembles that for a de-Laval nozzle. The upper two diagrams gives the pressure and velocity profiles for a neutral gas in such a de-Laval nozzle-like configuration. The solutions for an MHD fluid are essentially the same under condition (3): we must simply replace pressure by the total of hydrostatic pressure P_P and magnetic pressure P_B. The region 1 field-aligned current ($J_\parallel$) flows inside the cusp proper, a part with decreasing velocities in the poleward direction (cases (b) and (c)). The solution is highly dependent on the boundary conditions.

$M = u/a$

1

supersonic

case **a**

case **c**

case **b**

subsonic

subsonic

P_{total}

not directly connected to the ionosphere

directly connected to the ionosphere

case **b**

subsonic

M = 1

case **c**

supersonic

case **a**

Magnetosheath

High-Altitude Cusp

Mantle

Laval Nozzle

Magnetopause

throat

Mantle

?

Magnetosheath

Magnetic

Mantle

cusp

Indentation Region

Magneto-pause

Boundary Cusp (?)

Cusp Proper

Mantle Cusp

(b) The solar wind dynamic pressure influences the wave amplitude and hence influences heavily (non-linearly) the average cusp particle influx and its morphology. Since the magnetosonic wave is expected to form quickly, the response of the cusp morphology to changes in the solar wind conditions must be instantaneous.

(c) Numerical simulations (Yamauchi, 1994) and analytical studies (Yamauchi et al., 1993b) show that such a compressional structure simultaneously generates two pairs of oppositely-directed field-aligned currents (FACs) flowing in the same directions as the region 1 and region 0 FACs. Accordingly, we expect very quick response of the FAC system (and hence the ionospheric convection) to the solar wind variations. The predicted region 1 FAC is much more intense and confined than the region 0 FAC (Yamauchi et al., 1993b). Since intense FACs generate field-aligned potential drops (Knight, 1973), we also expect keV ion beams equatorward of the cusp.

(d) The predicted bow-shaped wave (Figure 1) is divided into a "nose" (center part where FACs are minimized) and two "wings" (dawn and dusk sides where FACs are generated). While the "nose" is rather stable, non-linear effects make the "wings" more active and variable with wake structures (Yamauchi, 1994). The quiet "nose" may correspond to the midday gap of aurora in the rather stable cusp proper. The wake may correspond to the multiple auroral arcs or the poleward moving transient aurorae which detach from the "cusp aurora" in the boundary cusp or the low-latitude boundary layer (LLBL).

(e) The breathing motion of the wave back and forth causes temporal changes of precipitation region, which result in multiple injections. The wake structure also produces multiple injections. Each injection is characterized by an energy-time dispersion under the velocity filter effect. If this motion is continuous, it causes a "slip" of the cusp boundary and may produce overlapping injections (Yamauchi et al., 1995, Figure 4). The wave may also jump upstream, especially for the "wing" part. This may result in discontinuous injections which gives the same low-altitude signatures as an FTE does. All these injections are smaller in scale size than the large-scale overall structure (cf. (a)), and these "meso-scale" structures are super-imposed on the large-scale quasi-steady cusp structure.

(f) In case the wave is standing, it produces only a single injection.

(g) The model requires a direct magnetosheath flow into the high-altitude cusp. Such a direct flow is expected to form in the magnetic cusp where the magnetic barrier is small, i.e., where $\beta \gg 1$ instead of rigid $B = 0$ (condition 3). The location of the magnetic cusp obey the IMF B_Y control as is predicted by the anti-parallel merging models (Crooker, 1979; Stasiewicz, 1991). Such a shift of the cusp position drastically changes the FAC distribution (Yamauchi and Lundin, 1992, Figure 4].

(h) Since the cusp particles originate at high-latitude but not at the equatorial region, the seasonal effect must be very strong because of the geometrical difference between winter- and summer-hemispheres with respect to the sun.

(i) Both the cusp-wave and the ionosphere may reflect the Alfvén waves travelling in between along the geomagnetic field (upward and downward dashed arrows in Figure 1). The upward Alfvén waves may trigger another detachment of the wake in Figure 1. The recurrence time of this magnetosphere-ionosphere (M-I) coupling process is a few minutes. The repeatedly reflected Alfvén wave forms a standing Alfvén wave at the place where the reflection is strongest, i.e., at the equatorward part of the cusp.

(j) The density of the cusp proper predicted in this model must be a little higher (but not by an order of magnitude) than that predicted by the cusp indentation model (Spreiter and Summers, 1967).

5 Comparison to Observations

We now compare these predictions with the low- and mid-altitude cusp observations during southward IMF. First, the ionospheric projection of Figure 1 agrees with the statistical overall morphology of the cusp-cleft region obtained by low-altitude and mid-altitude satellites (Kremser and Lundin, 1990; Newell and Meng, 1992; and references therein). The other observations are also consistent with the predictions:

1. The solar wind dynamic pressure radically affects the cusp morphology (Newell and Meng, 1994; Yamauchi et al., 1996) (cf. (b)).

2. The ion data displays large-scale energy-time (enregy-latitude) dispersion (Burch et al., 1982; Yamauchi and Lundin, 1994) (cf. (a)).

3. The ion energy-time (enregy-latitude?) dispersion is sometimes characterized by a single entry (Reiff et al., 1977), and more often by a multiple entry (Norberg et al., 1994) (cf. (e) and (f)).

4. The multiple ion entry shows sometimes a "wash board" signature, sometimes an "overlapping injection" signature, and sometimes but rarely a "staircase" signature (Escoubet et al., 1992; Norberg et al., 1994) (cf. (e)).

5. The multiple ion entry is, if observed by mid-altitude satellites, often seen as small-scale temporal ion injections embedded into the large-scale spatial structure (Yamauchi and Lundin, 1994). The former is characterized by ion energy-time dispersion while the latter by ion energy-latitude dispersion (Yamauchi and Lundin, 1994) (cf. (e)), although the "wash board" cases observed at low altitudes do not easily fit this interpretation (Norberg et al., 1994).

6. The overlapping injections are observed by both low- and mid-altitude satellites (Yamauchi and Lundin, 1994; Norberg et al., 1994) (cf. (e)).

7. The large-scale cusp morphology is very stable despite the intrusion of many smaller-scale structures (Yamauchi and Lundin, 1994) (cf. (a), (d) and (e)).

8. The latitudinal width of the cusp is sometimes extended and sometimes narrow. The IMF direction and plasma pressure apparently control this (Newell and Meng, 1987, 1994) (cf. (b)); however, a variety of cusp sizes can be found for similar solar wind conditions (Yamauchi and Lundin, 1994) (cf. (d)).

9. The region of the most intense particle precipitation moves continuously ("slipping") rather than by a jump (Nilsson et al., 1996) (cf. (d) and (e)).

10. Co-populated with cusp particles, large-scale FACs (cusp-part region 1 FAC and mantle FAC) are found near local noon forming paired FACs in both the prenoon and postnoon sides (McDiarmid et al., 1979; Erlandson et al., 1988; Yamauchi et al., 1993a) (cf. (c)).

11. The cusp location and the large-scale FAC distribution are strongly correlated to the IMF B_Y component [e.g., Friis-Christensen et al., 1985; Erlandson et al., 1988; Newell et al., 1989) (cf. (g)). The present model also predicts a correlation between the cusp position and the azimuthal deflection of the solar wind if IMF B_Y is negligible (a dawnward deflection shifts the cusp location duskward) although this is not well studied.

12. The large-scale FAC distribution, the ionospheric convection, and the large-scale cusp morphology instantaneously respond to changes in the solar wind conditions (Clauer and Banks, 1986; Yamauchi et al., 1995) (cf. (b) and (c)).

13. There are strong seasonal effects in both the particle precipitation (Newell and Meng, 1988) and the FAC intensity (Yamauchi and Araki, 1989) exclusively in the cusp. They cannot be explained by a difference in the ionospheric conductivity only (cf. (h)).

14. The cusp aurora normally has a midday gap (Dandekar and Pike, 1978; Murphree et al., 1980; Meng and Lundin, 1986) (cf. (d)).

15. Poleward moving auroral transients are observed detaching from cusp/cleft aurora especially when the cusp is moving southward (Sandholt et al., 1994, and references therein). They are observed east or west of the cusp proper (Minow et al., 1994) (cf. (d)).

16. The repetition time of the transient auroral forms, originally interpreted to be about 10 minutes, is now found to be normally about a few minutes (Fasel et al., 1994) (cf. (i)).

17. Waves and turbulence are more intensified in the boundary cusp than in the cusp proper (Marklund et al., 1990; Pottelette et al., 1990) (cf. (a)).

18. Standing Alfvén waves are observed in the same region (Maynard et al., 1991) (cf. (i)).

19. Substantial heating of ions to several hundred eV is observed in the boundary cusp compared to the cusp proper (Woch and Lundin, 1992) (cf. (a)).

20. Local field-aligned acceleration up to about 1 keV is observed at the equatorward-most boundary of the cusp (Woch and Lundin, 1992) (cf. (c)). The electrons are also simultaneously accelerated there, but this is probably due to wave turbulence (e.g., André et al., 1990) (cf. (a) and (c)) because electron spikes are often attained only at low altitudes but not at mid altitudes according to DE-1 and DE-2 comparison (Naito, 1988).

21. Hill and Reiff (1977) derived the field-aligned component of the source ion bulk velocity to be about 500 km/s. A more careful analysis using a better resolution data showed a much lower value (100 km/s) (Woch and Lundin, 1992). The result cannot be used in support of or against any cusp models.

22. Ionospheric convection (e.g., Heppner and Maynard, 1987; Woch and Lundin, 1992) is a result of an electrostatic potential (or space charge) distribution. So, an appropriate distribution of FACs automatically provides appropriate ionospheric convection in general (cf. (c), (d) and (g)). On the other hand, it is not easy to quantitatively predict the convection velocity at the all altitude because the convection velocity is not necessarily conserved inside the same flux tube (Yamauchi and Blomberg, 1997). For example, the "overlapping injection" events (point 6) imply that there must be at least two different convection velocities for plasma on the same field lines. Furthermore, if we have open and closed patches at the magnetopause boundary (Sanchez and Siscoe, 1990), space charges accumulated on the scattered closed patches may significantly modify the global potential distribution.

6   Conclusion

The wave-assisted cusp model (or Laval-nozzle cusp model) depicted in Figure 1 (a standing compressional structure is formed at the foremost part of the high-altitude cusp) is consistent with many low- and mid-altitude cusp observations during southward IMF. The model is theoretically feasible under the following major assumptions: 1. A direct plasma flow exists from the magnetosheath to the plasma mantle through the high-altitude cusp, and there is a sufficient plasma supply from the ionosphere to the plasma mantle. 2. The magnetic tension force in this flow does not break down significantly the mass-, momentum-, and energy-conservation laws. Two physical mechanisms, namely the narrowing of the "stream tube" due to the special geometry (Laval nozzle effect) and the seeding of magnetospheric/ionospheric plasma downstream (mixture effect) reinforce each other to form a local compressional region in the high-altitude cusp.

References

André, M., Crew, G.B., Peterson, W.K., Persoon, A.M., Pollock, C.J., and Engebretson, M.J., Ion heating by broadband low-frequency waves in the cusp/cleft, *J. Geophys. Res.*, *95*, 20809–20823, 1990.

Burch, J.L., Reiff, P.H., Heelis, R.A., Winningham, J.D., Hanson, W.B., Gurgiolo, C., Menietti, J.D., Hoffman, R.A., and Barfield, J.N., Plasma injection and transport in the mid-altitude polar cusp, *Geophys. Res. Lett.*, *9*, 921–924, 1982.

Clauer, C.R., and Banks, P.M., Relationship of the interplanetary electric field to the high-latitude ionospheric electric field and currents: Observations and model simulation, *J. Geophys. Res.*, *91*, 6959–6971, 1986.

Courant, R., and Friedrichs, K.O., Supersonic flow and shock waves, 464pp, Interscience, New York, 1948.

Dandekar, B.S., and Pike, C.P., The midday discrete auroral gap, *J. Geophys. Res.*, *83*, 4227–4236, 1978.

Erlandson, R.E., Zanetti, L.J., Potemra, T.A., Bythrow, P.F., and Lundin, R., IMF BY dependence of region 1 Birkeland currents near noon, *J. Geophys. Res.*, *93*, 9804–9814, 1988

Escoubet, C.P., Smith, M.F., Fung, S.F., Anderson, P.C., Hoffman, R.A., Basinska, E.M., and Bosqued, J.M., Staircase ion signature in the polar cusp: A case study, *Geophys. Res. Lett.*, *19*, 1735–1738, 1992.

Fasel, G.J., Minow, J.I., Lee, L.C., Smith, R.W. and Deehr, C.S., Poleward-moving auroral forms: what do we really know about them, Transient dayside auroral forms: what do we really know about them?, in *Physical Signatures of Magnetospheric Boundary Layer Processes*, edited by J. A. Holtet, and A. Egeland, pp. 211–226, Kluwer academic press, Dordrecht, 1994.

Friis-Christensen, E., Kamide, Y., Richmond, A.D., and Matsushita, S., Interplanetary magnetic field control of high-latitude electric fields and currents determined from Greenland magnetometer data, *J. Geophys. Res.*, *90*, 1325–1338, 1985.

Heppner, J.P., and Maynard, N.C., Empirical high-latitude electric field models, *J. Geophys. Res.*, *92*, 4467–4489, 1987.

Hill, T.W., and Reiff, P.H., Evidence of magnetospheric cusp proton acceleration by magnetic merging at the dayside magnetopause, *J. Geophys. Res.*, *82*, 3623–3628, 1977.

Knight, S., Parallel electric fields, *Planet. Space Sci., 21*, 741–750, 1973.

Kremser, G., and Lundin, R., Average spatial distributions of energetic particles in the mid-altitude cusp/cleft region observed by Viking, *J. Geophys. Res.*, *95*, 5753–5766, 1990.

Marklund, G.T., Blomberg, L.G., Flthammar, C.-G., Erlandson, R.E., and Potemra, T.A., Signatures of the high-altitude polar cusp and dayside auroral regions as seen by the Viking electric field experiment, *J. Geophys. Res.*, *95*, 5767–5780, 1990.

Maynard, N.C., Aggson, T.L., Basinska, E.M., Burke, W.J., Craven, P., Peterson, W.K., Sugiura, M., and Weimer, D.R., Magnetospheric boundary dynamics: DE-1 and DE-2 observations near the magnetopause and cusp, *J. Geophys. Res.*, *96*, 3505–3522, 1991.

McDiarmid, I.B., Burrows, J.R., and Wilson, M.D., Large-scale magnetic field perturbations and particle measurements at 1400 km on the dayside, *J. Geophys. Res.*, *84*, 1431–1441, 1979.

Meng, C.-I., and Lundin, R., Auroral morphology of the midday oval, *J. Geophys. Res.*, *91*, 1572–1584, 1986.

Minow, J.I., Smith, R.W., Denig, W.F., and Newell, P.T., Dayside auroral dynamics during reconfiguration of the auroral oval, in *Physical Signatures of Magnetospheric Boundary Layer Processes*, edited by J. A. Holtet, and A. Egeland, pp. 201–210, Kluwer academic press, Dordrecht, 1994.

Murphree, J.S., Cogger, L.L., Anger, C.D., Ismail, S., and Shepherd, G.G., Large scale 6300 , 5577 , 3914 dayside auroral morphology, *Geophys. Res. Lett.*, *7*, 239–242, 1980.

Naito, H., *En-jiryokusen denryu no teiryoteki kaiseki* (Qauntita-tive analyses of the field-aligned currents), Master thesis (in Japanese), Faculty of Science, Kyoto University, Japan, 1988.

Newell, P.T., and Meng, C.-I., Cusp width and B_Z: Observations and a conceptual model, *J. Geophys. Res.*, *92*, 13673–13678, 1987.

Newell, P.T., and Meng, C.-I., Hemispherical asymmetry in cusp precipitation near solstices, *J. Geophys. Res.*, *93*, 2643–2648, 1988.

Newell, P.T., and Meng, C.-I., Mapping the dayside ionosphere to the magnetosphere according to particle precipitation characteristics, *Geophys. Res. Lett.*, *19*, 609–612, 1992.

Newell, P.T., and Meng, C.-I., Ionospheric projections of magnetospheric regions under low and high solar wind pressure conditions, *J. Geophys. Res.*, *99*, 273–286, 1994.

Newell, P.T., Meng, C.-I., Sibeck, D.G., and Lepping, R., Some low-altitude cusp dependencies on the interplanetary magnetic field, *J. Geophys. Res.*, *94*, 8921–8927, 1989.

Nilsson, H., Yamauchi, M., Eliasson, L., Norberg, O., and Clemmons, J., The ionospheric signature of the cusp as seen by incoherent scatter radar, *J. Geophys. Res.*, *101*, 10947–10963, 1996.

Norberg, O., Yamauchi, M., Eliasson, L., and Lundin, R., Freja observations of multiple injection events in the cusp, *Geophys. Res. Lett.*, *21*, 1919–1922, 1994.

Podgorny, I.M., Dubilin, E.M., and Potanin, Y.N., The magnetic field on the magnetospheric boundary from laboratory simulation data, *Geophys. Res. Lett.*, *5*, 207–210, 1978.

Pottelette, R., Malingre, M., Dubouloz, N., Aparicio, B., Lundin, R., Holmgren, G., and Marklund, G., High-frequency waves in the cusp/cleft regions, *J. Geophys. Res.*, *95*, 5957–5971, 1990.

Reiff, P.H., Hill, T.W., and Burch, J.L., Solar wind plasma injection at the dayside magnetospheric cusp, *J. Geophys. Res.*, *82*, 479–491, 1977.

Sanchez, E.R., and Siscoe, G.L., IMP 8 magnetotail boundary crossings: a test of the MHD models for an open magnetosphere, *J. Geophys. Res.*, *95*, 20771–20779, 1990.

Sandholt, P.E., Farrugia, C.J., Burlaga, L.F., Holtet, J.A., Moen, J., Lybekk, B., Jacobsen, B., Opsvik, D., Egeland, A., Lepping, R., Lazarus, A.J., Hansen, T., Brekke, A., and Friis-Christensen, E., Cusp/cleft auroral activity in relation to solar wind dynamic pressure, interplanetary magnetic field B_Z and B_Y, *J. Geophys. Res.*, *99*, 17323–17342, 1994.

Sckopke, N., Paschmann, G., Rosenbauer, H., and Fairfield, D.H., Influence of the interplanetary magnetic field on the occurrence and thickness of the plasma mantle, *J. Geophys. Res.*, *81*, 2687–2691, 1976.

Spreiter, J.R., and Summers, A.L., On conditions near the neutral points on the magnetosphere boundary, *Planet. Space Sci., 15*, 787–798, 1967.

Stasiewicz, K., A global model of gyroviscous field line merging at the magnetopause, *J. Geophys. Res.*, *96*, 77–86, 1991.

Walters, G.K., On the existence of a second standing shock wave attached to the magnetosphere, *J. Geophys. Res.*, *71*, 1341–1344, 1966.

Woch, J., and Lundin, R., Magnetosheath plasma precipitation in the polar cusp and its control by the interplanetary magnetic field, *J. Geophys. Res.*, *97*, 1421–1430, 1992.

Yamauchi, M., Numerical simulation of large-scale field-aligned currents generation from finite-amplitude magnetosonic waves, *Geophys. Res. Lett.*, *21*, 851–854, 1994.

Yamauchi, M., and Araki, T., The interplanetary magnetic field B_Y-dependent field-aligned current in the dayside polar cap under quiet conditions, *J. Geophys. Res.*, *94*, 2684–2690, 1989.

Yamauchi, M., and Lundin, R., A new cusp model and its Viking observation (in Japanese with English abstract), in *3rd STEP Report*, 782pp, edited by H. Oya, 666–672, Sendai, Japan, 1992.

Yamauchi, M., and Lundin, R., Classification of large-scale and meso-scale ion dispersion patterns observed by Viking over the

cusp-mantle region, in *Physical Signatures of Magnetospheric Boundary Layer Processes*, edited by J. A. Holtet, and A. Egeland, pp. 99–109, Kluwer academic press, Dordrecht, 1994.

Yamauchi, M., and Blomberg, L., Problems on Mappings of the Convection and on the Fluid Concept, *Phys. Chem. Earth*, this issue, 1997.

Yamauchi, M., Lundin, R., and Woch, J., The interplanetary magnetic field B_Y effects on large-scale field-aligned currents near local noon: Contributions from cusp part and noncusp part, *J. Geophys. Res.*, *98*, 5761–5767, 1993a.

Yamauchi, M., Lundin, R., and Lui, A.T.Y., Vorticity equation for MHD fast waves in geospace environment, *J. Geophys. Res.*, *98*, 13523–13528, 1993b.

Yamauchi M., Lundin, R., and Potemra, T.A., Dynamic response of the cusp morphology to the IMF changes: An example observed by Viking, *J. Geophys. Res.*, *100*, 7661–7670, 1995.

Yamauchi, M., Nilsson, H., Eliasson, L., Norberg, O., Boehm, M., Clemmons, J.H., Lepping, R.P., Blomberg, L., Ohtani, S., Yamamoto, T., Mukai, T., Terasawa, T., and Kokubun, S., Dynamic response of the cusp morphology to the solar wind: A case study during passage of the solar wind plasma cloud on February 21, 1994, *J. Geophys. Res.*, *101*, 24675–24687, 1996.